Supporting Information

Control of Spin Coupling Through Redox-active Bridge in Dinickel(II) Porphyrin Dimer: Step-wise Oxidations Enable Isolations of the Chlorin-porphyrin Heterodimer and Dication Diradical with Singlet Ground State

Younis Ahmad Pandit, Mohammad Usman, Anindya Sarkar, Syed Jehanger Shah, and Sankar Prasad Rath*

Department of Chemistry, Indian Institute of Technology Kanpur, Kanpur-208016, INDIA. Email: sprath@iitk.ac.in

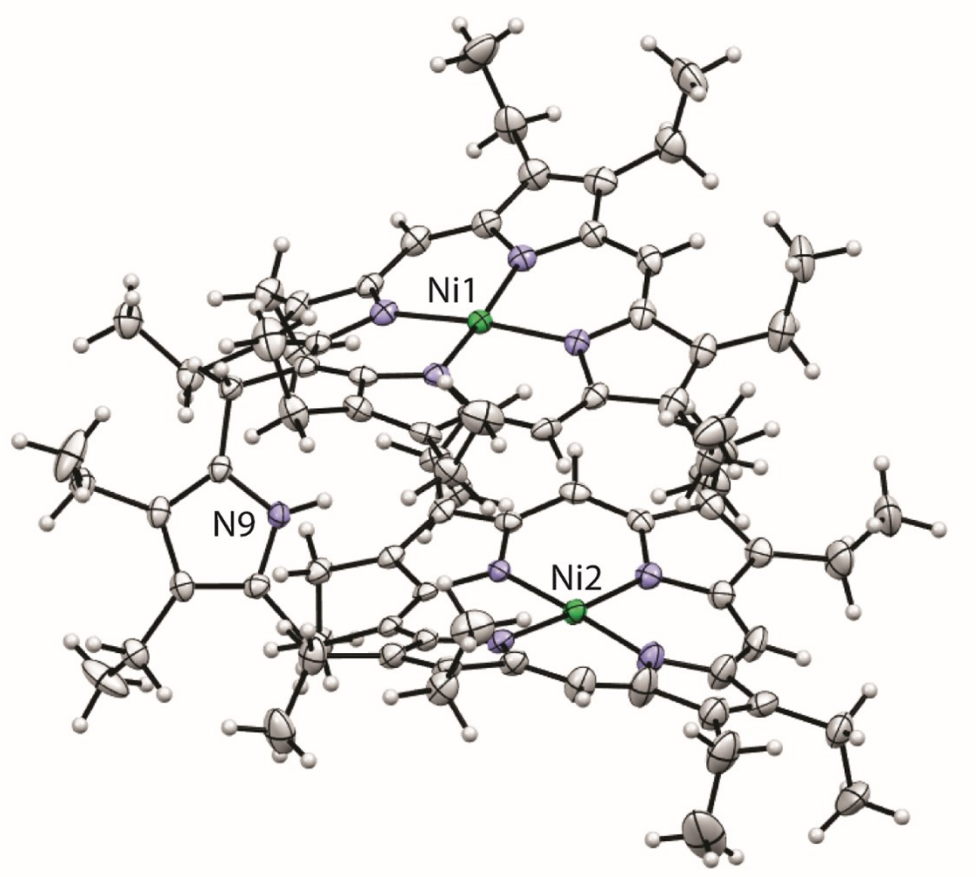

Fig. S1. An ORTEP diagram (at 100 K) of **1**•Ni showing thermal ellipsoids at the 50% probability level for non-hydrogen atoms.

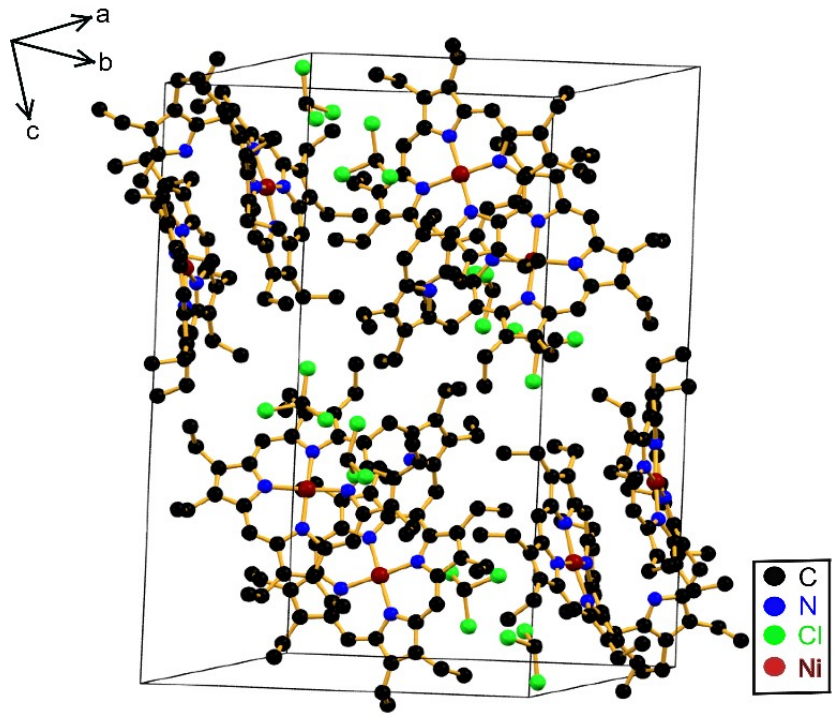

Fig. S2. Diagram depicting the molecular packing of **1**•Ni.2CHCl$_3$ in the unit cell (H-atoms have been omitted for clarity).

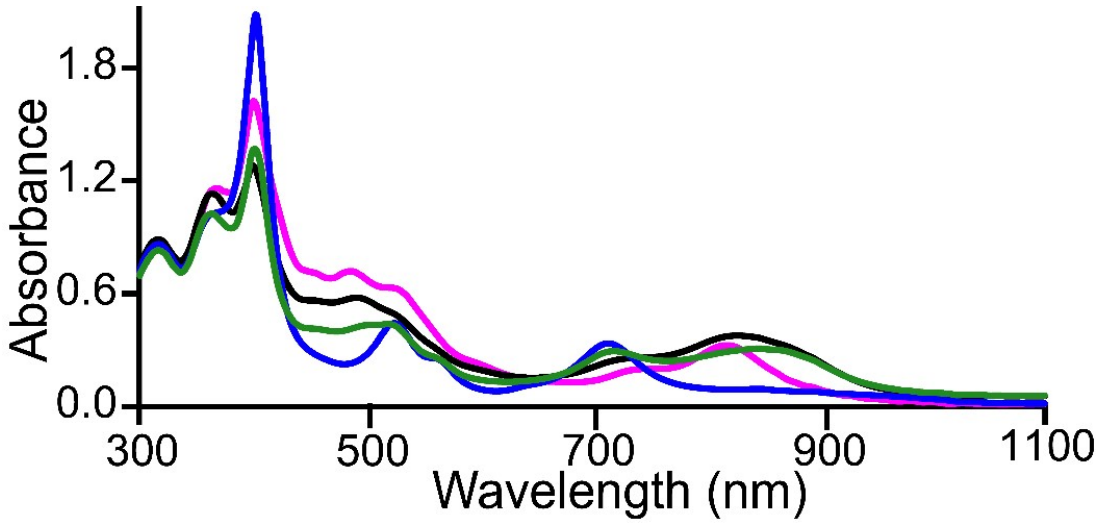

Figure S3. UV-vis-NIR (in CH_2Cl_2 at 295 K) spectral changes recorded at different time intervals upon standing of **1**•Ni•DDQ in air.

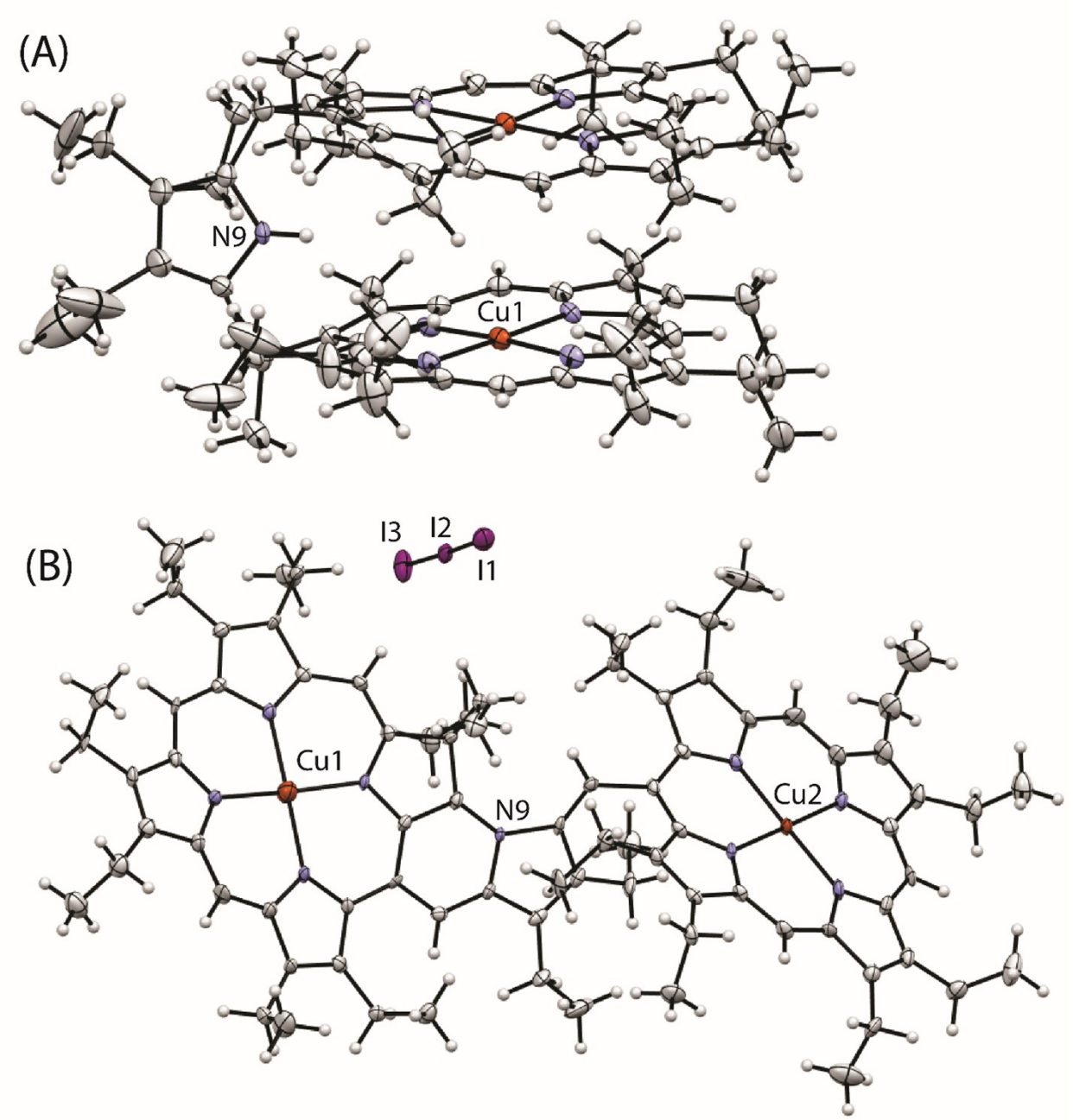

Fig. S4. ORTEP diagrams (at 100 K) of (A) **1**•Cu and (B) **2**•Cu•I_3 showing thermal ellipsoids at the 50% probability level for non-hydrogen atoms.

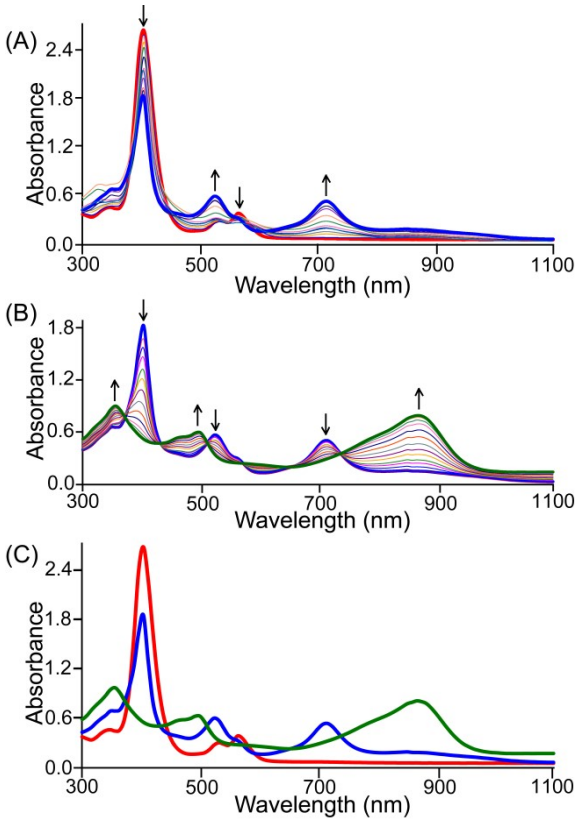

Figure S5. UV-vis-NIR (in CH_2Cl_2 at 295 K) spectral change of 2.0 x 10^{-5} M solution of **1**•Ni upon addition of (A) 0 to 1.0 eq. and (B) 1.0 to 2.0 eq. of $AgSbF_6$. (C) Comparison of UV-vis-NIR spectra (in CH_2Cl_2 at 295 K) of **1**•Ni (red line), **3**•Ni•SbF_6 (blue line) and **4**•Ni•$(SbF_6)_2$ (green line).

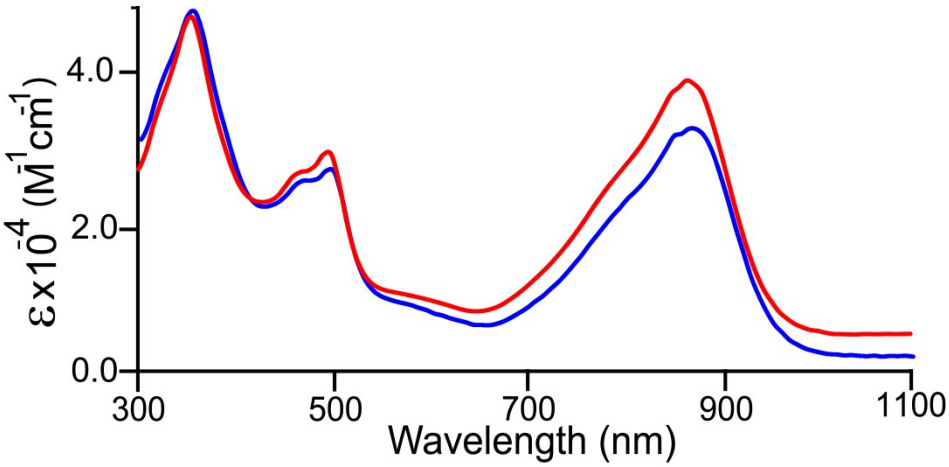

Figure S6. Comparative UV-vis-NIR spectra (in CH_2Cl_2 at 295 K) of **4**•Ni•$(FeCl_4)_2$ (blue line) and **4**•Ni•$(SbF_6)_2$ (red line).

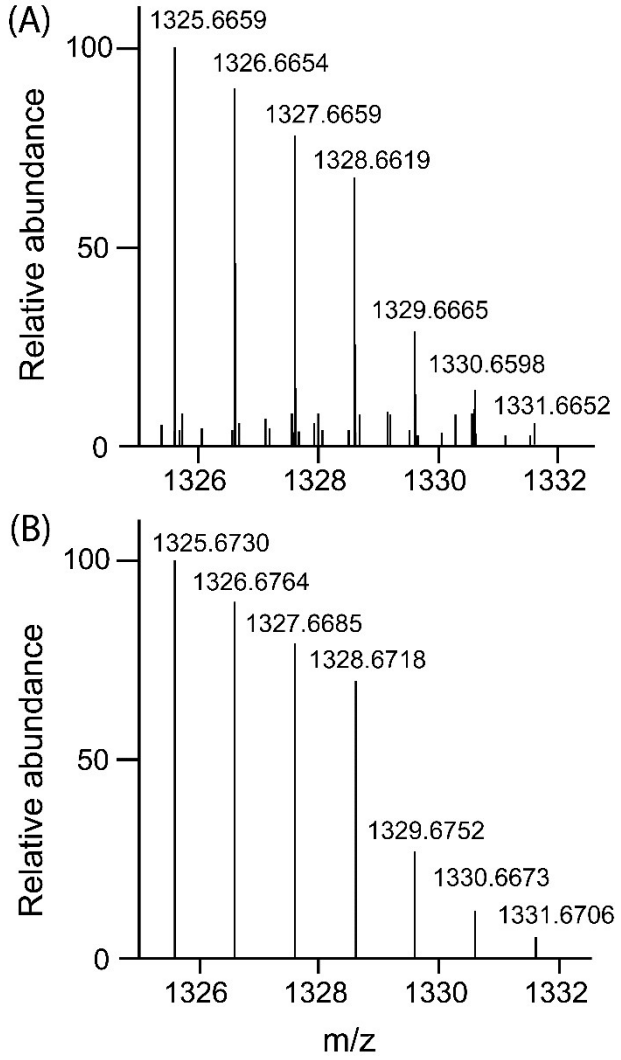

Figure S7. Isotopic distribution of the (A) experimental and (B) simulated ESI mass spectrum (positive-ion mode) of [**2**•Ni•DDQ +H]$^{+}$.

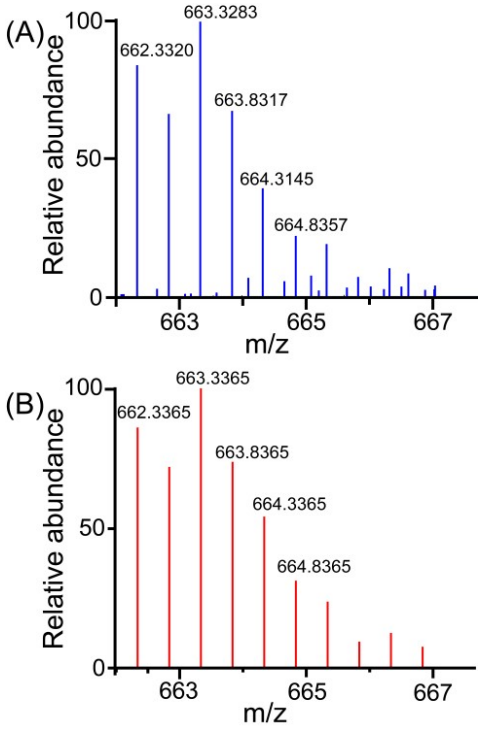

Figure S8. Isotopic distribution of the (A) experimental and (B) simulated ESI mass spectrum (positive-ion mode) of [**4**•Ni]$^{2+}$.

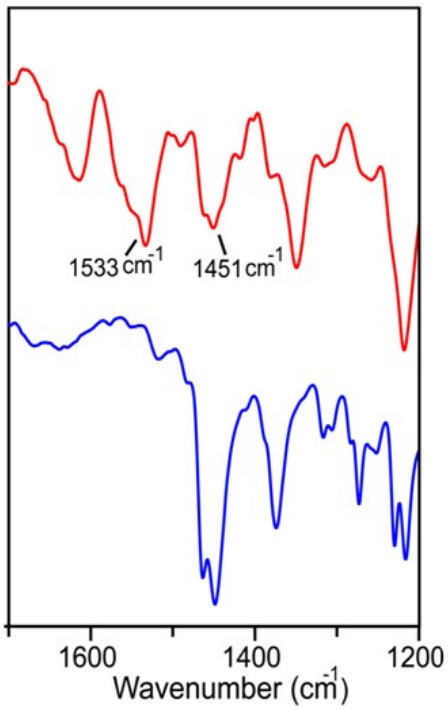

Figure S9. FT-IR spectra (at 295 K) (selected portions only) of solid polycrystalline samples of **1**•Ni (blue line) and **4**•Ni•$(FeCl_4)_2$ (red line). The π-cation radical marker bands in **4**•Ni•$(FeCl_4)_2$ have been labelled.

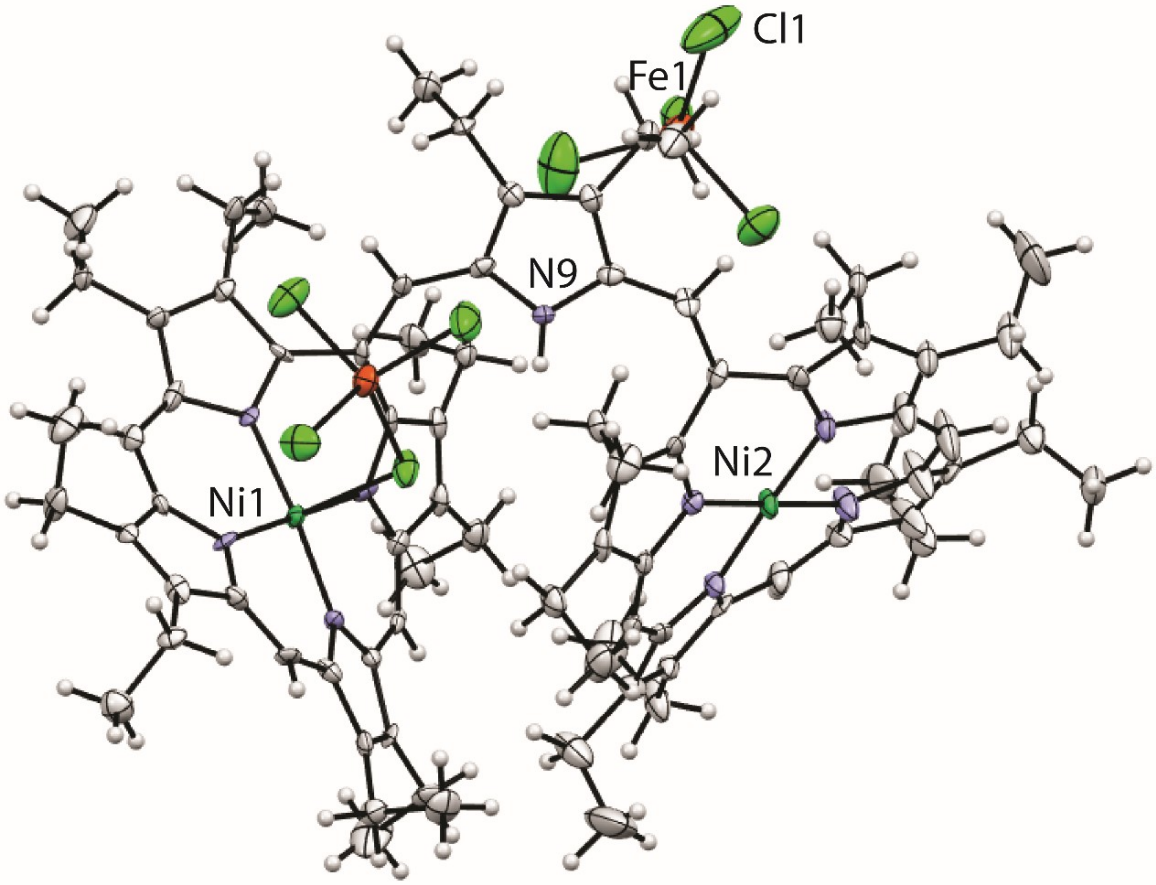

Fig. S10. An ORTEP diagram (at 100 K) of **4**•Ni•$(FeCl_4)_2$ showing thermal ellipsoids at the 50% probability level for non-hydrogen atoms.

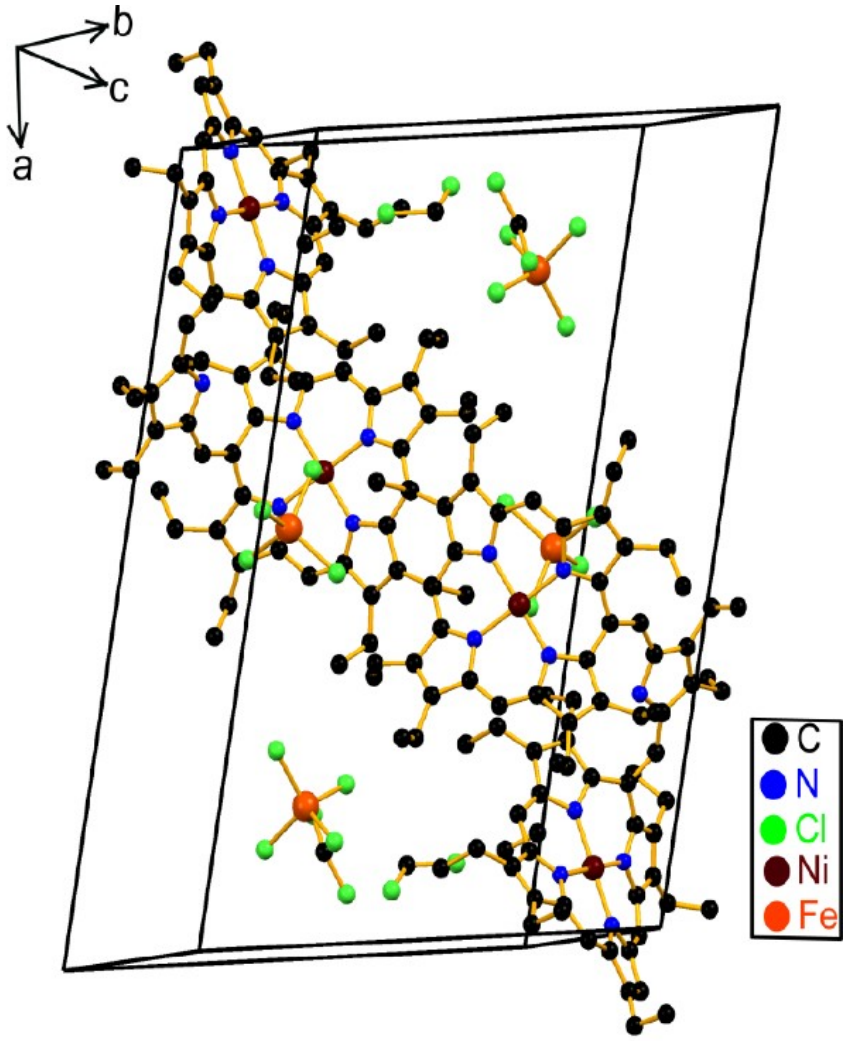

Fig. S11. Diagram depicting the molecular packing of **4**•Ni•$(FeCl_4)_2$.$2CH_2Cl_2$ in the unit cell (H-atoms have been omitted for clarity).

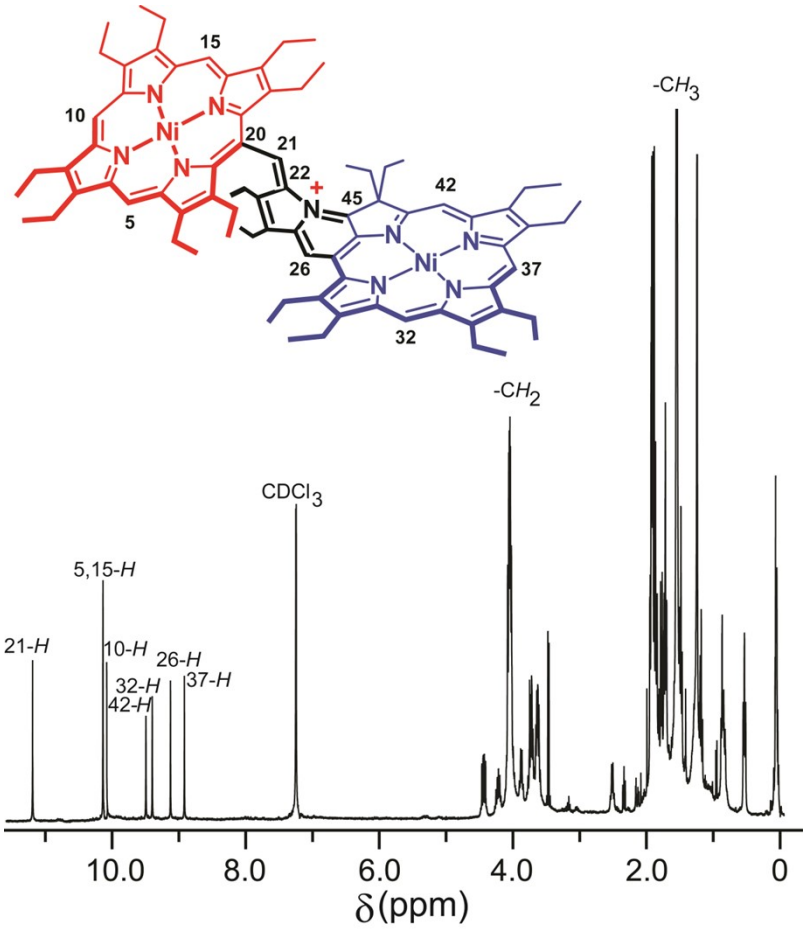

Fig. S12. ^{1}H NMR spectra (in $CDCl_3$ at 295 K) of **2**•Ni•DDQ.